Evolution of the phase diagram of LaFeP$_{1-x}$As$_x$O$_{1-y}$F$_y$ ($y = 0$–0.1)

K. T. Lai,[1] A. Takemori,[1] S. Miyasaka,[1,*] F. Engetsu,[2] H. Mukuda,[2] and S. Tajima[1]

[1]*Department of Physics, Osaka University, Osaka 560-0043, Japan*
[2]*Graduate School of Engineering Science, Osaka University, Osaka 560-8531, Japan*

P/As substitution effects on the transport properties of polycrystalline LaFeP$_{1-x}$As$_x$O$_{1-y}$F$_y$ with $x = 0$–1.0 and $y = 0$–0.1 have been studied. In the F-free samples ($y = 0$), a superconducting (SC) dome with a maximum T_c of 12 K is observed around $x = 0$–0.3. This is separated from another SC dome with $T_c \sim 10$ K at $x = 0.6$–0.8 by an antiferromagnetic region ($x = 0.3$–0.6), giving a two-dome feature in the $T_c - x$ phase diagram. As y increases, the two SC domes merge together, changing to a double-peak structure at $y = 0.05$ and a single dome at $y = 0.1$. This proves the presence of two different Fermi surface states in this system.

I. INTRODUCTION

Since the discovery of iron-based superconductors, one of the focuses is to find a unified picture of the electronic state among various kinds of iron-based superconductors. It has been revealed that the suppression of spin density wave (SDW) in their parent compounds is important to induce high-T_c superconductivity (SC) in most of the cases. For example, hole-doped (Ba,K)Fe$_2$As$_2$ [1], electron-doped Ba(Fe,Co)$_2$As$_2$ [2], and isovalent-element–doped BaFe$_2$(As,P)$_2$ [3] share a similar phase diagram which shows the transition from SDW to SC state upon doping. This similarity suggests that the spin fluctuation (SF) near a quantum critical point (QCP) is a possible candidate for the pairing force of Cooper pairs. In LaFeAsO, however, the phase diagram is much more complicated. For example, in LaFeAs(O,H) [4,5], as H content increases after the suppression of SDW, two SC regions have been observed in the phase diagram, as well as the reappearance of an antiferromagnetic (AFM) phase in the overdoped region. The origin of these interesting behaviors has been argued in relation to SF or orbital fluctuations [5–9].

On the other hand, LaFePO is known as a superconductor with $T_c \sim 5$ K without any trace of SDW [10,11]. Introducing electrons by F substitution cannot change T_c significantly [12]. The striking difference between the properties of the two parent compounds LaFeAsO and LaFePO raises a question about its origin and the relation to SC. Experimental observations [13–17] and theoretical calculations [18–22] have shown that the Fermi surface (FS) topologies of LaFeAsO and LaFePO are different, mainly in one of the hole pockets. In particular, the two-dimensional (2D) FS exists in LaFeAsO around the X point, while the three-dimensional (3D) FS around the Z point exists in LaFePO. The difference in the resulting FS nesting may be related to the different SC behaviors.

P/As substitution in LaFe(As,P)O provides a platform for studying the relationship among SC, AFM, and corresponding FS nesting. A study of LaFe(As,P)O in P doping level from 0% to 60% has been reported previously [23]. After the suppression of SDW around LaFeAsO, a SC dome with a

maximum critical temperature $T_c \sim 10$ K appears at around 30% P doping. Recently, a further study from the NMR technique has indicated the AFM ordering at around 50% P doping with $T_N \sim 15$ K [24]. Such complex behaviors suggest the importance of the role of AFM correlation to induce SC in LaFe(As,P)O.

In our previous work, we have also studied the P/As substitution effect in the same system but for 10% F doping, namely, LaFeP$_{1-x}$As$_x$O$_{0.9}$F$_{0.1}$ [25–27]. A maximum $T_c \sim 28$ K has been observed at $x = 0.6$, together with temperature (T), linearly dependent resistivity, and a strong T-dependent Hall coefficient. It suggests that SF is strong at around $x = 0.6$, which has been confirmed in the NMR study [28]. Moreover, it has been revealed that this anomaly at $x = 0.6$ is commonly observed not only in La-1111 systems, but also in Nd-1111 and Pr-1111 systems which are different in lattice sizes. This implies that the important electronic change, presumably a band crossover, is driven by P/As substitution.

As described above, LaFePO and LaFeAsO systems have different FS states because of the existence of a d_{Z^2} or $d_{X^2-Y^2}$ band near the Fermi level. The P/As substitution causes the exchange of the energy level of the $d_{Z^2}/d_{X^2-Y^2}$ band. Consequently, our previous results show the anomalous behaviors, suggesting that RFeP$_{1-x}$As$_x$O$_{0.9}$F$_{0.1}$ ($R =$ La, Pr, and Nd) has the FeP-type FS below $x \sim 0.6$, while the samples of $x = 1.0$ have FeAs-type FS. However, the evidence of our scenario (two FS states and the band crossover around $x = 0.6$) was weak.

In this study, we have extended our previous work to lower F content ($y = 0$ and 0.05). The transport properties for LaFeP$_{1-x}$As$_x$O$_{1-y}$F$_y$ with $y = 0$ and 0.05 have been mainly studied, and we have tried to clarify the phase diagram, which provides further evidence for the presence of two electronic states originating from the two different FS topologies and their crossover.

II. EXPERIMENTAL METHODS AND SAMPLE CHARACTERIZATION

Polycrystalline LaFeP$_{1-x}$As$_x$O$_{1-y}$F$_y$ with nominal $x = 0$–1 and $y = 0$, 0.05 were synthesized by a solid-state reaction method. The precursors LaAs/LaP, Fe$_2$O$_3$, Fe, and LaF$_3$ were mixed and pressed into pellets. The pellets were sealed in evacuated quartz tubes and heated at 1100 °C for 40 h. All the
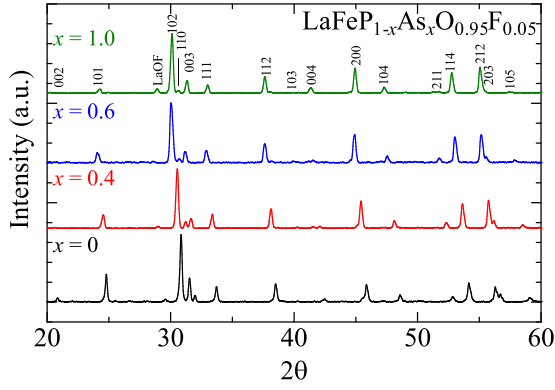
*miyasaka@phys.sci.osaka-u.ac.jp

FIG. 1. (Color online) The x-ray diffraction patterns of LaFeP$_{1-x}$As$_x$O$_{0.95}$F$_{0.05}$ ($x = 0$, 0.4, 0.6, and 1.0). Almost all the peaks are able to be indexed assuming the $P4/nmm$ tetragonal symmetry.

above processes except heating were performed in a glove box with pure Ar environment.

The crystal structure was characterized by powder x-ray diffraction with the source of Cu K_α radiation at room temperature. Magnetic susceptibility measurements were performed in a Quantum Design Magnetic Property Measurement System (MPMS) with an applied field of 10 Oe. The electrical resistivity was measured by a standard four-probe method. Hall effect measurements were performed in the magnetic field up to 7 T. R_H was obtained from Hall resistivity, which showed linear dependence on the magnetic applied field. The ^{31}P-NMR spectra in the AFM phase were measured by sweeping the magnetic field to determine the transition temperature T_N [29].

The typical powder x-ray diffraction patterns for $y = 0.05$ are shown in Fig. 1. Almost all the Bragg peaks observed in the diffraction patterns are able to be assigned within the tetragonal $P4/nmm$ symmetry. Note that a minor impurity peak of LaOF is found in some samples. The corresponding lattice constants a and c for the samples of $y = 0$ and 0.05 are calculated by the least-squares fitting of the Bragg peaks and the data is plotted in Fig. 2. Both samples for $y = 0$ and 0.05 show a linear increase in a and c with increasing As content x.
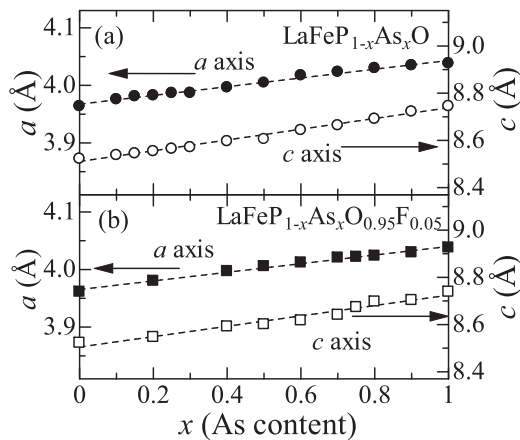

FIG. 2. The x dependence of the lattice constants a and c of (a) LaFeP$_{1-x}$As$_x$O and (b) LaFeP$_{1-x}$As$_x$O$_{0.95}$F$_{0.05}$.
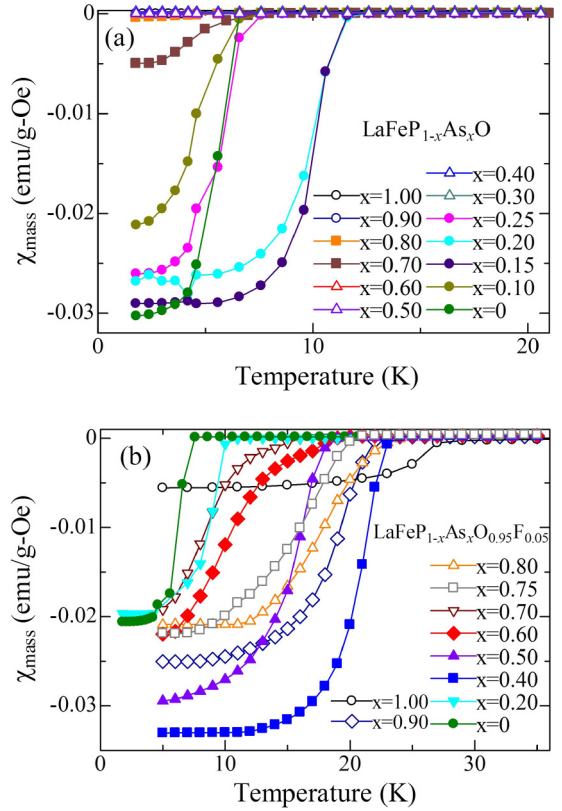

FIG. 3. (Color online) The temperature dependence of magnetic susceptibility of (a) LaFeP$_{1-x}$As$_x$O and (b) LaFeP$_{1-x}$As$_x$O$_{0.95}$F$_{0.05}$.

This linear change of lattice constants indicates that the As/P solution compounds are successfully prepared.

In order to determine the actual As and F concentrations, we performed the energy-dispersive x-ray spectroscopy (EDX) measurements. The result of EDX indicates that the actual As concentration is the same as the nominal one (x) in all the samples. On the other hand, we are not able to estimate the actual F concentration by EDX measurements, because there are peaks for La and Fe near the peak for F in the EDX spectrum. With increasing the nominal F concentration y, however, the lattice constants a and c continuously decrease. (Please see Fig. 2 and Ref. [27].) In the previous report, we have roughly estimated the actual F concentration of $\sim$0.03–0.04 in the samples with the nominal F concentration $y = 0.1$ [27]. Assuming that the lattice constants depend linearly on the actual F concentration, the actual F concentration is about 0.01 in the samples with nominal F concentration of $y = 0.05$. In short, we can determine the actual As concentration and not the actual F concentration by EDX measurements. For convenience, we use the nominal F concentration ($y = 0$ and 0.05) in this paper.

III. RESULTS AND DISCUSSION

Figure 3 shows the T dependence of magnetic susceptibility for the $y = 0$ and 0.05 samples. The SC transition can be observed in all the samples of $y = 0.05$, and the samples of $y = 0$ with $x = 0$–0.25, 0.7, and 0.8. Note that the
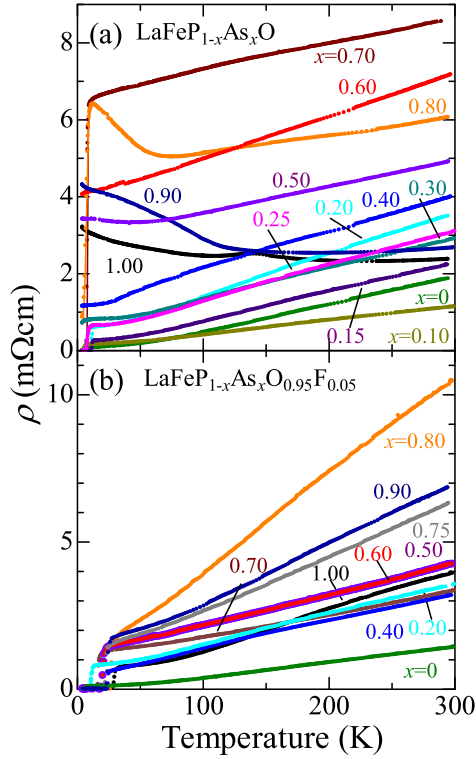
FIG. 4. (Color online) The temperature dependence of the electrical resistivity of (a) $LaFeP_{1-x}As_xO$ and (b) $LaFeP_{1-x}As_xO_{0.95}F_{0.05}$ with various values of x, respectively.

FIG. 5. (Color online) The As-doping x dependence of (a) critical temperature T_c, Néel temperature T_N of $LaFeP_{1-x}As_xO$, (b) T_c of $LaFeP_{1-x}As_xO_{0.95}F_{0.05}$, (c) T_c of $LaFeP_{1-x}As_xO_{0.9}F_{0.1}$, and (d) the exponent n in $\rho(T) = \rho_0 + AT^n$ of $LaFeP_{1-x}As_xO_{1-y}F_y$. T_c is determined by both zero resistivity and the onset of the drop in magnetic susceptibility. The open circles are the data by Wang *et al.* [23] and Kitagawa *et al.* [24].

superconducting volume fraction of the samples of $x = 0.7$ and 0.8 for $y = 0$ is much smaller than the other SC samples.

Figure 4 shows the T dependence of resistivity $\rho(T)$ for the $y = 0$ and 0.05 samples. The SC transition can be observed in all the SC samples identified in the magnetic susceptibility measurement. In the $y = 0$ samples, the anomalous upturn in $\rho(T)$ is observed for $x = 0.8$–1 due to the SDW transition, which determines T_N. The $x = 0.3$–0.6 samples seemingly behave as normal metals, but the $x = 0.5$ sample shows an upturn at low T (<50 K), which may be related to the recently reported AFM phase [24]. Actually we observe the broadening of NMR spectra at $x = 0.3$–0.6, which indicates the existence of AFM ordering [29]. We suppose that the behaviors of resistivity obtained in these polycrystalline samples are dominated mainly by the ab-plane resistivity ρ_{ab} due to the large ratio of the c-axis resistivity ρ_c to ρ_{ab}. In fact, the large anisotropy ratio ρ_c/ρ_{ab} ($\sim$20–200) was reported by resistivity measurements of single-crystalline LaFeAsO [30].

T_c and T_N of all the samples for $y = 0$ are summarized in Fig. 5(a). For $y = 0$, two SC domes and two AFM phases are observed in the phase diagram. The values of T_c at $x = 0.6$–0.8 (SC1 dome) are consistent with the previous study [23]. The other SC dome at $x = 0$–0.3 (SC2 dome) is found in the present study. The maximum T_c of the SC2 dome is slightly higher ($\sim$12 K) than that of the SC1 dome. Between the two SC domes, an AFM order (AFM2 phase) is detected via the NMR technique [24,29], with T_N ranging from $\sim$15 to 35 K. Another AFM phase (AFM1 phase) is also observed above $x = 0.8$ through $\rho(T)$ and NMR [24]. Here the AFM order is accompanied with a structural phase transition. The values of
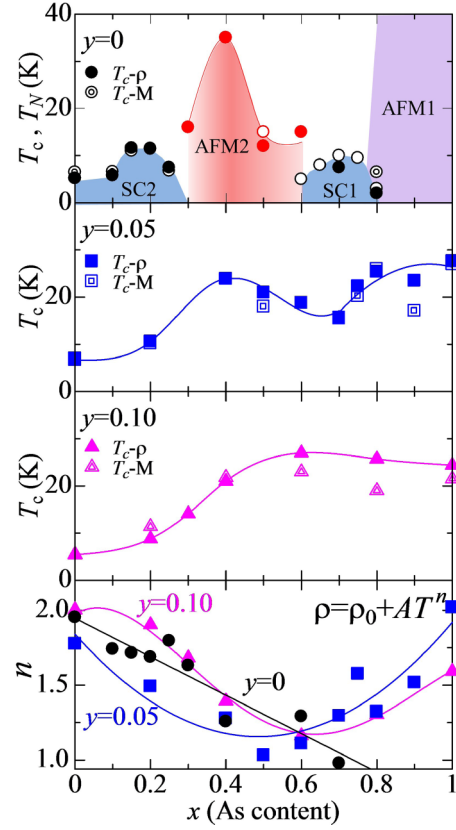
T_N, between $\sim$50 and 140 K, in the AFM1 phase are much higher than those in the AFM2 phase.

Figure 5(b) shows the x dependence of T_c for $y = 0.05$. A local minimum of $T_c(x)$ is found around $x = 0.6$, giving a double-peak structure. If we further increase y to 0.1 [27], as illustrated in Fig. 5(c), only a single peak is observed at $x = 0.6$. These results suggest that the two SC domes found at $y = 0$ merge with each other when y increases.

The exponent n of $\rho(T)$ is determined by fitting the data with $\rho(T) = \rho_0 + AT^n$, where ρ_0 is the residual resistivity and A is the slope of $\rho(T)$. The range of fitting is between T just above T_c and $\sim$100 K. As shown in Fig. 5(d), for the series of $y = 0$, n changes gradually from 2 to 1 when x increases to 0.7. Note that the data of $x = 0.5$, 0.8–1.0 are not suitable for fitting because of the upturn at low T. Roughly speaking, the value of n is close to 2 in the SC2 dome while it is $\sim$1 in the SC1 dome, suggesting that the behavior of $\rho(T)$ near the SC2 dome is described as a Fermi liquid (FL) while that near the SC1 dome is non-FL. Since the $x = 0.7$ sample is near the boundary of the SDW phase, the gradual decrease in n with increasing x suggests the existence of a QCP around $x = 0.7$. This point of view is consistent with the previous theoretical prediction [31]. It is rather surprising that the AFM
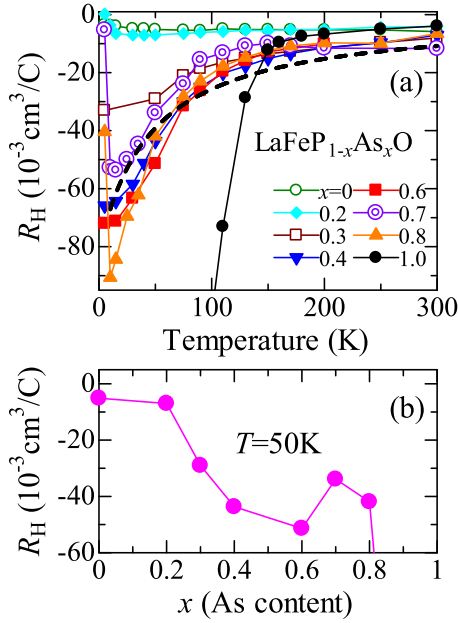
FIG. 6. (Color online) (a) The temperature dependence of the Hall coefficient R_H of LaFeP$_{1-x}$As$_x$O with various x. The dashed curve is the fitting of the data for $x = 0.4$, for example, by using the equation $R_H = -\alpha_0/(T + \Theta)$. (b) The x dependence of R_H at 50 K for LaFeP$_{1-x}$As$_x$O.

order observed in NMR does not seriously affect the behaviors in resistivity.

For both series of y = 0.05 and 0.1, the value of n approaches 1 at around $x = 0.6$, and 2 at $x = 0$ for both series of $y = 0.05$ and 0.1. This indicates that both systems exhibit non-FL behavior at around $x = 0.6$, while they behave as FL at around $x = 0$.

Since the Hall coefficient R_H is sensitive to the change of electronic states, it has also been measured for LaFeP$_{1-x}$As$_x$O. Figure 6(a) illustrates T dependence of R_H for the series of $y = 0$. For $x = 0$ and 0.2, $|R_H|$ is very small and almost T independent, which is consistent with the FL picture suggested by the measurements of resistivity. When x exceeds 0.3, R_H begins to show a strong T dependence, namely, $|R_H|$ is strongly enhanced at low T and suddenly drops at T_c. Although this low-T enhancement of $|R_H|$ is weakened once at $x = 0.7$, it increases again at $x \geqslant 0.8$. A large drop of R_H observed around 140 K at $x = 1$ indicates the appearance of SDW, which is consistent with the $\rho(T)$ data and the previous studies [23,32].

To visualize the correspondence to the phase diagram in Fig. 5(a), we plot the x dependence of R_H at 50 K in Fig. 6(b), as a measure of strength of T dependence of R_H. Here we can find that the SC2 dome ($0 \leqslant x \leqslant 0.25$) shows a weak T dependence of R_H, while the AFM2 phase ($0.3 < x < 0.6$) exhibits a strong T dependence. Although the decrease in R_H is slightly recovered at $x = 0.7$ in SC1 dome, R_H drops again in the AFM1 phase above $x = 0.8$.

The origin of the strong T dependence of R_H in the intermediate x region may be explained by the following two aspects. The first one is related to the change of FS through P/As substitution. The band calculation [20] has demonstrated that the main difference between FS topology of LaFeAsO and LaFePO is the hole pocket located at ($\pi,\pi,0$), named the

γ pocket. Since the $d_{X^2-Y^2}$ band dominates the FS at (π,π,z) across $z = 0 - \pi$ (2D tubelike FS), the γ pocket is observable in LaFeAsO. On the other hand, in LaFePO, the d_{Z^2} band which replaces from $d_{X^2-Y^2}$ touches the Fermi level only around (π,π,π) but not ($\pi,\pi,0$), forming a 3D FS pocket. Therefore the γ pocket in the $k_z = 0$ plane is absent in LaFePO. If As is substituted by P, the energy of the $d_{X^2-Y^2}$ and d_{Z^2} bands will interchange, and as a result the γ pocket will shrink in size and finally vanish. We believe that this reconstruction of FS affects the T dependence of R_H. According to the results in Fig. 6, the interchange of FS topology is supposed to happen between $x = 0.3$ and 0.8. Following the discussion about the presence of two different kinds of electronic states and their crossover in LaFeP$_{1-x}$As$_x$O$_{0.9}$F$_{0.1}$ in our previous study [27], we expect that there are two electronic states corresponding to two types of FS topology and the crossover of these two states causes the enhancement of $|R_H|$.

The second aspect is related to the AFM phase between $x = 0.3$ and 0.6. Since the AFM order may create a charge gap in some part of the FS, it may decrease the number of charge carriers and thus enhance $|R_H|$ at low T. Another fact is that the T-dependent R_H of these samples can be roughly fitted with the equation $R_H = -\alpha_0/(T + \Theta)$, α_0 and Θ being constants, which is derived from the SF theory [33,34]. This relation suggests that the strong T dependence of $|R_H|$ is related to the presence of the backflow due to strong electron-electron scattering arising from SF, which is consistent with the observation of low-energy SF above T_N in these samples via NMR technique [24,29]. Therefore the enhancement of $|R_H|$ at $x = 0.3$–0.6 may be correlated to the AFM order in AFM2 phase. A small decrease in R_H at $x = 0.7$ indicates a recovery of FS which gives SC.

The second aspect, however, cannot be adopted in the case of the F-doped system with $y = 0.1$ [27]. Although a similar enhancement of $|R_H|$ is observed near $x = 0.6$, the electronic state is far from the AFM order. Therefore the anomaly in R_H near $x = 0.6$ for the series of $y = 0.1$ should be attributed to the band crossover (the first aspect).

Finally, we discuss the evolution of the electronic properties in LaFeP$_{1-x}$As$_x$O$_{1-y}$F$_y$. The phase diagram of this system is illustrated in Fig. 7, which demonstrates the evolution of a two-SC-dome feature. The two-dome structure at $y = 0$ becomes a single-dome structure at $y = 0.1$. It can be viewed as the expansion of a SC2 dome with increasing y as a result of the suppression of AFM2 phase through F doping. The SF originating from the AFM2 phase contributes to the development of SC at $x \sim 0.4$ in the series of $y = 0.05$. In the series of $y = 0.1$, the As content for the maximum strength of SF and the maximum value of T_c is shifted to $x = 0.6$. It suggests that the SC2 dome further expands and merges with the SC1 dome, resulting in a single dome.

It is clear that the enhancement of T_c in the SC2 dome (or in the lower x region) is commonly due to the increase of SF suggested by the change of T dependence of $\rho(T)$, namely, the decrease of the exponent n from 2. The enhancement of SF from the FL state has also been observed by NMR experiments [28,29]. Therefore the SC in the low-x region is more likely to be induced by SF. In contrast, there is no clear correlation between T_c and the exponent n in the larger x (As-rich) region.
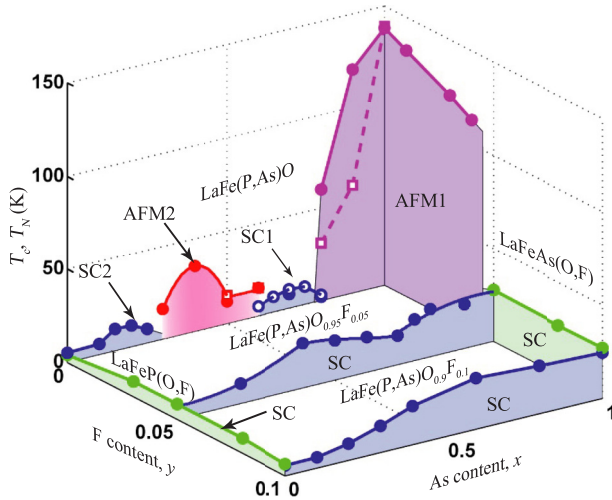
FIG. 7. (Color online) The phase diagram of LaFeP$_{1-x}$As$_x$O$_{1-y}$F$_y$ [12,27,35]. The open dots indicate the data by Wang *et al.* [23] and Kitagawa *et al.* [24].

Here we note that the exponent n approaches $\sim$1 around $x = 0.6$ in all y series [see Fig. 2(d)]. Although the band crossover is suggested in the region of $0.3 \leqslant x \leqslant 0.8$ for $y = 0$ and at $x \sim 0.6$ for $y = 0.1$ by the Hall effect measurements, there is no theoretical model that connects the T-linear $\rho(T)$ and band crossover. This, together with the SC mechanism in the larger x region, remains a puzzle.

IV. CONCLUSION

We have studied the transport properties of polycrystalline LaFeP$_{1-x}$As$_x$O$_{1-y}$F$_y$ from $y = 0$–0.1. For $y = 0$, an SC dome (SC2 dome) has been found at $x = 0$–0.3, constructing a two-dome structure in the phase diagram. With increasing y, the SC2 dome expands and merges with the SC1 dome. Consequently, it results in a double-peak structure of $T_c(x)$ in the series of $y = 0.05$ and a single SC dome in the series of $y = 0.1$. In addition to the AFM phase near LaFeAsO, another AFM phase is observed at $x = 0.3$–0.6 (AFM2 phase) via NMR in the series of $y = 0$. A strong temperature dependence of R_H observed in the AFM2 phase suggests the AFM order opens a charge gap at some parts of the FS. F doping suppresses the AFM order in the AFM2 phase and the residual SF induces SC, causing expansion of the SC2 dome. The temperature dependence of $\rho(T)$ commonly approaches T linear at $x \sim 0.6$ in all y series, together with the strong T dependence of R_H. The evolution of the two SC domes could strongly support the scenario that there exist two different electronic states corresponding to the two FS topologies for the P-rich and the As-rich compositions, respectively. To clarify the SC mechanism for the latter composition regions, further studies are required.

[1] M. Rotter, M. Pangerl, M. Tegel, and D. Johrendt, Angew. Chem. Int. Ed. **47**, 7949 (2008).

[2] J.-H. Chu, J. G. Analytis, C. Kucharczyk, and I. R. Fisher, Phys. Rev. B **79**, 014506 (2009).

[3] S. Kasahara *et al.*, Phys. Rev. B **81**, 184519 (2010).

[4] S. Iimura, S. Matuishi, H. Sato, T. Hanna, Y. Muraba, S. W. Kim, J. E. Kim, M. Takata, and Hideo Hosono, Nat. Commun. **3**, 943 (2012).

[5] N. Fujiwara, S. Tsutsumi, S. Iimura, S. Matsuishi, H. Hosono, Y. Yamakawa, and H. Kontani, Phys. Rev. Lett. **111**, 097002 (2013).

[6] S. Iimura *et al.*, Phys. Rev. B **88**, 060501(R) (2013).

[7] Y. Yamakawa, S. Onari, H. Kontani, N. Fujiwara, S. Iimura, and H. Hosono, Phys. Rev. B **88**, 041106(R) (2013).

[8] K. Suzuki, H. Usui, K. Kuroki, S. Iimura, Y. Sato, S. Mstsuishi, and H. Hosono, J. Phys. Soc. Jpn. **82**, 083702 (2013).

[9] S. Onari, Y. Yamakawa, and H. Kontani, Phys. Rev. Lett. **112**, 187001 (2014).

[10] Y. Kamihara, H. Hiramatsu, M. Hirano, R. Kawamura, H. Yanagi, T. Kamiya, and H. Hosono, J. Am. Chem. Soc. **128**, 10012 (2006).

[11] J. J. Hamlin, R. E. Baumbach, D. A. Zocco, T. A. Sayles, and M. B. Maple, J. Phys.: Condens. Matter **20**, 365220 (2008).

[12] S. Suzuki, S. Miyasaka, S. Tajima, T. Kida, and M. Hagiwara, J. Phys. Soc. Jpn. **78**, 114712 (2009).

[13] A. I. Coldea, J. D. Fletcher, A. Carrington, J. G. Analytis, A. F. Bangura, J.-H. Chu, A. S. Erickson, I. R. Fisher, N. E. Hussey, and R. D. McDonald, Phys. Rev. Lett. **101**, 216402 (2008).

[14] H. Sugawara, R. Settai, Y. Doi, H. Muranaka, K. Katayama, H. Yamagami, and Y. Onuki, J. Phys. Soc. Jpn. **77**, 113711 (2008).

[15] C. Liu, Y. Lee, A. D. Palczewski, J.-Q. Yan, T. Kondo, B. N. Harmon, R. W. McCallum, T. A. Lograsso, and A. Kaminski, Phys. Rev. B **82**, 075135 (2010).

[16] D. H. Lu, M. Yi, S.-K. Mo, J. G. Analytis, J.-H. Chu, A. S. Erickson, D. J. Singh, Z. Hussain, T. H. Geballe, I. R. Fisher, and Z.-X. Shen, Physica C **469**, 452 (2009).

[17] D. H. Lu, M. Yi, S.-K. Mo, A. S. Erickson, J. Analytis, J.-H. Chu, D. J. Singh, Z. Hussain, T. H. Geballe, I. R. Fisher, and Z.-X. Shen, Nature (London) **455**, 81 (2008).

[18] S. Lebègue, Phys. Rev. B **75**, 035110 (2007).

[19] D. J. Singh and M.-H. Du, Phys. Rev. Lett. **100**, 237003 (2008).

[20] K. Kuroki, H. Usui, S. Onari, R. Arita, and H. Aoki, Phys. Rev. B **79**, 224511 (2009).

[21] V. Vildosola, L. Pourovskii, R. Arita, S. Biermann, and A. Georges, Phys. Rev. B **78**, 064518 (2008).

[22] R. Thomale, C. Platt, W. Hanke, and B. A. Bernevig, Phys. Rev. Lett. **106**, 187003 (2011).

[23] C. Wang, S. Jiang, Q. Tao, Z. Ren, Y. Li, L. Li, C. Feng, J. Dai, G. Cao, and Z. A. Xu, Europhys. Lett. **86**, 47002 (2009).

[24] S. Kitagawa, T. Iye, Y. Nakia, K. Ishida, C. Wang, G.-H. Cao, and Z.-A. Xu, J. Phys. Soc. Jpn. **83**, 023707 (2014).

[25] S. Saijo, S. Suzuki, S. Miyasaka, and S. Tajima, Physica C **470**, S298 (2010).

[26] S. Miyasaka, A. Takemori, S. Saijo, S. Suzuki, and S. Tajima, J. Phys. Chem. Solid **72**, 414 (2011).

[27] S. Miyasaka, A. Takemori, T. Kobayashi, S. Suzuki, S. Saijo, and S. Tajima, J. Phys. Soc. Jpn. **82**, 124706 (2013).

[28] H. Mukuda, F. Engetsu, K. Yamamoto, K. T. Lai, M. Yashima, Y. Kitaoka, A. Takemori, S. Miyasaka, and S. Tajima, Phys. Rev. B **89**, 064511 (2014).

[29] H. Mukuda, F. Engetsu, T. Shiota, K. T. Lai, M. Yashima, Y. Kitaoka, S. Miyasaka, and S. Tajima, J. Phys. Soc. Jpn. **83**, 083702 (2014).

[30] A. Jesche, F. Nitsche, S. Probst, Th. Doert, P. Müller, and M. Ruck, Phys. Rev. B **86**, 134511 (2012).

[31] J. Dai, Q. Si, J.-X. Zhu, and E. Abrahams, Proc. Natl. Acad. Sci. USA **106**, 4118 (2009).

[32] I. Pallecchi, F. Bernardini, F. Caglieris, A. Palenzona, S. Massidda, and M. Putti, Eur. Phys. J. B **86**, 338 (2013).

[33] H. Kontani, K. Kanki, and K. Ueda, Phys. Rev. B **59**, 14723 (1999).

[34] Y. Nakajima, H. Shishido, H. Nakai, T. Shibauchi, K. Behnia, K. Izawa, M. Hedo, Y. Uwatoko, T. Matsumoto, R. Settai, Y. Ōnuki, H. Kontani, and Y. Matsuda, J. Phys. Soc. Jpn. **76**, 024703 (2007).

[35] H. Luetkens, H.-H. Klauss, M. Kraken, F. J. Litterst, T. Dellmann, R. Klingeler, C. Hess, R. Khasanov, A. Amato, C. Baines, M. Kosmala, O. J. Schumann, M. Braden, J. Hamann-Borrero, N. Leps, A. Kondrat, G. Behr, J. Werner, and B. Büchner, Nat. Mater. **8**, 305 (2009).